CHEMBIOCHEM

DOI: 10.1002/cbic.200700590

Globotriose-Functionalized Gold Nanoparticles as Multivalent Probes for Shiga-like Toxin

Yuh-Yih Chien,[a, b] Mi-Dan Jan,[c] Avijit Kumar Adak,[c] Hsiao-Chien Tzeng,[d] Yen-Ping Lin,[d] Yu-Ju Chen,[a] Ken-Tseng Wang,[b] Chien-Tien Chen,[d] Chia-Chun Chen,*[d] and Chun-Cheng Lin*[a, c]

Compared to monovalent carbohydrates, multivalent carbohydrate ligands exhibit significantly enhanced binding affinities to their interacting proteins. Here, we report globotriose (P^k ligand)-functionalized gold nanoparticle (AuNP) probes for the investigation of multivalent interactions with the B_5 subunit of Shiga-like toxin I (B-Slt). Six P^k-ligand-encapsulated AuNPs (P^k-AuNPs) of varying particle size and linker length were synthesized and evaluated for their potential as multivalent affinity probes by using a surface plasmon resonance competition assay. The affinity of these probes for the interacting proteins was greatly affected by nanoparticle size, linker length, and ligand density on nanoparticle surface. For example, the 20-nm 20-P^k-I-AuNP, which had a relatively long linker showed a $>10^8$-fold increase in affinity compared with the mono P^k ligand. This intrinsic high-affinity AuNP probe specifically captured the recombinant B-Slt from Escherichia coli *lysate, and the resulting purity of the B-Slt was $>95\%$. We also developed a robust P^k-AuNP-based detection method for Slt-I by combining the technique with silver enhancement.*

Introduction

With the aid of synthetic multivalent ligands, the concept of multivalency in carbohydrate–protein interactions at interfaces is now well established.[1] Although the interaction between single carbohydrate and protein molecules is weak ($K_a = 10^3$–$10^4\ M^{-1}$), nature overcomes this problem by the multivalent presentation of receptors and ligands to achieve high-affinity binding with high specificity.[2] As a consequence of such multivalent binding sites, multiple distinct ligands often simultaneously bind with high affinity to receptors, and thus such ligands might serve as antagonists/agonists for multiple receptors.[3] A variety of diverse scaffolds have been formulated for multivalent ligand presentation,[4] including dendrimers,[5] polymers,[6] liposomes,[7] and globular proteins,[8] or engineered molecular scaffolds.[9] The power of chemical synthesis makes synthetic multivalent ligands available as valuable probes for studying receptor function.[10]

The shiga and shiga-like toxins (Slts) are a family of classic AB_5-type bacterial toxins that contain a single enzymatically active A-subunit, and five copies of a B-subunit. The radially symmetric B-subunit pentamer (B-Slt) that is produced by *Escherichia coli* O157:H7 specifically recognizes globotriaosylceramide (Gb_3).[11] The Gb_3 glycolipid is known as the globotriose (P^k) blood group antigen or CD77,[12,13] which contains the trisaccharide αGal(1→4)βGal(1→4)βGlc.[14] Slts cause gastrointestinal diseases after entering mammalian cells through multivalent binding of the B-subunit to the saccharide portion of glycolipids on the cell surface. The X-ray crystal structure of B-Slt[15] has shown that there are 15 binding sites on this protein complex that engage the cell surface P^k antigens over a 6-nm diameter area. Recently, two high-affinity multivalent inhibitors for bacterial toxins were designed and synthesized, and these inhibitors use different binding mechanisms.[16,17] In a pioneering contribution, Bundle et al. designed a promising inhibitor for shiga-like toxin I (Slt-I) by conjugating the P^k trisaccharide ligand on a starfish-like multivalent ligand carrier, and showed a million-fold increase in activity that resulted from the effective binding of five of 15 binding sites of B-Slt and the formation of a hamburger-like complex.[17] Toone et al. developed bivalent C-linked P^k-trisaccharide-based glycopeptides as affinity ligands for B-Slt in microcalorimetry studies.[18] Inhibition of B-Slt binding to cells has been demonstrated to protect mice from infection by *E. coli* O157:H7.[19] Thus, it could be of great benefit to develop both a B-Slt antagonist to protect against *E. coli* infection, and a sensitive, accurate and rapid assay to detect the toxin.[20–22]

In recent decades, gold nanoparticles (AuNPs) that are functionalized with biomolecules have been developed and widely

[a] *Y.-Y. Chien, Prof. Y.-J. Chen, Prof. C.-C. Lin*
Institute of Chemistry, and Genomics Research Centre, Academia Sinica
128 Taipei (Taiwan)
Fax: (+886) 3-5711082
E-mail: cclin66@mx.nthu.edu.tw

[b] *Y.-Y. Chien, K.-T. Wang*
Department of Chemistry, National Taiwan University
106 Taipei (Taiwan)

[c] *M.-D. Jan, Dr. A. K. Adak, Prof. C.-C. Lin*
Department of Chemistry, National Tsing Hua University
300 Hsinchu (Taiwan)

[d] *H.-C. Tzeng, Y.-P. Lin, Prof. C.-T. Chen, Prof. C.-C. Chen*
Department of Chemistry, National Taiwan Normal University
116 Taipei (Taiwan)

Supporting information for this article is available on the WWW under http://www.chembiochem.org or from the author.

used as model systems for biological interaction studies and biolabels.[23] Self-assembled monolayers of thiolated glycoconjugates on gold surfaces are of particular interest.[24,25] In early studies, Penadés et al. initiated the use of AuNPs as multivalent ligand carriers and synthesized trisaccharide Le^x AuNPs for studies of carbohydrate–carbohydrate interactions.[26] The thiolated glycoconjugates are relatively easy to assemble on the gold surface through a Au–S covalent bond, and the size of the AuNP can be specified by varying the reaction conditions. These gold glyconanoparticles have been used successfully as carriers to present carbohydrate ligands for studying carbohydrate–protein and carbohydrate–carbohydrate interactions.[27–32]

Previously, we demonstrated the labeling of a specific protein on the bacterial cell surface by using mannose-conjugated AuNPs (m-AuNP).[33] m-AuNPs were used to visualize the position of individual *FimH* proteins on the type 1 pilus of *E. coli* by using electron microscopy. Moreover, this concept has been extended to the quantitative analysis of multivalent interactions between a tetrameric plant lectin, concanavalin A (Con A), and several different carbohydrate-AuNPs.[34] These experiments demonstrated that the binding of Con A to m-AuNP is enhanced dramatically (by ~100-fold) compared with binding to free mannose. Also, we have explored the identification of a target protein from a protein mixture by using galactose and P^k-coated AuNPs in combination with MALDI-TOF MS.[35] By using this nanoprobe-based mass spectrometry approach, the target lectin PA-IL was identified at femtomole concentrations, and its discontinuous binding epitopes were revealed simultaneously.

Although the development of multivalent carbohydrate ligands for Slt-I through inhibitory or antagonistic modes has attracted significant attention from investigators, only a few such ligands have been designed that interact with all of the B-subunit binding sites simultaneously.[16,17] Therefore, a more thorough understanding of multivalent complex formation is desirable to further advance strategies for design of multivalent ligands. Herein, we used P^k-conjugated AuNPs (P^k-AuNP) as probes to study multivalent interactions with B-Slt. A surface plasmon resonance (SPR) competition binding assay[36,37] was applied to investigate the binding affinity of P^k-AuNPs for B-Slt. Our results have allowed us to develop: 1) a water-soluble 20-P^k-I-AuNP antagonist for B-Slt that shows $>10^8$-fold binding affinity enhancement over the monovalent P^k trisaccharide ligand, 2) P^k-AuNPs affinity probes to extract B-Slt from bacterial cell lysate with high purity (>95%) while maintaining its activity, and 3) a P^k-AuNP-based detection assay for Slt-I.

Results and Discussion

Synthesis of P^k antigen

Compounds **1** and **2**[35] are P^k antigens that contain a linker of two different lengths, and **1** and **2** were synthesized as we previously described,[38] with modifications, as shown in Scheme 1. Previously, we used lactoside **4** and galactosyl phosphite donor **5** to construct the P^k trisaccharide derivative **6**. However, undesirable glycosidic bond cleavage occurred during the oxidation of the terminal double bond in **3** to generate a carboxyl group in **4**. Thus, in this study, the carboxyl group was introduced at the early stage of the synthesis of **6**. Ruthenium-trichloride-catalyzed oxidation of the olefin moiety in **7** was followed by esterification to give **8**,[39] which was transformed to **9** by following our previous procedure.[38] To link the P^k trisaccharide onto AuNP, a thiol functionality was needed in compound **9**. Compound **1** was obtained by coupling **9** with ethylene glycol linker **10**, and then by treating the resulting product with thioacetic acid, followed by global deacetylation. Compound **2** was obtained according to our previous report.[35]

Fabrication of P^k-conjugated AuNPs

To synthesize various sizes (4, 13, and 20 nm) of P^k-AuNPs, $NaBH_4$, and sodium citrate were chosen as the reducing reagents. The size of the resulting AuNPs depended on the reactivity of reducing agent and its concentration in an aqueous solution of tetrachloroauric acid ($HAuCl_4$). The 4-nm P^k-conjugated AuNP (4-s-P^k-AuNP) was prepared by a modified Brust's procedure[40] by using $HAuCl_4$, $NaBH_4$, and the P^k-**2** dimer. To synthesize larger P^k-AuNPs, the AuNPs were first prepared by using 148 μM $HAuCl_4$ and 34 μM sodium citrate solution to give 13-nm AuNPs; the use of a higher concentration of $HAuCl_4$ (296 μM) gave 20-nm AuNPs.[41] The surface sodium citrate of 13 and 20 nm AuNPs was then exchanged with P^k ligand **2** in the presence of $NaBH_4$ to afford 13-s-P^k-AuNP and 20-s-P^k-AuNP, respectively. Similarly, compound **1**, which had the longer linker, was assembled on AuNPs of different sizes to give 4-l-, 13-l-, and 20-l-P^k-AuNPs. Transmission electron microscopy (TEM) images showed that the P^k-AuNPs were spherical with average diameters of 4.0 ± 1.0 nm (4-s-P^k-AuNPs), 13.3 ± 2.1 nm (13-s-P^k-AuNPs) and 20.6 ± 4.1 nm (20-s-P^k-AuNPs; Figure 1). The UV-visible spectra of the AuNPs before and after coupling with P^k clearly showed characteristic plasmon absorption bands at 517, 525 and 528 nm (see Figure S1 in the Supporting Information) for 4-, 13-, and 20-nm AuNPs, respectively. The lack of a red-shift of the band after modification also indicated that no aggregation occurred in aqueous media. These P^k-AuNPs were stable at 4°C for at least 6 months. This strategy allowed us to modify the surface carbohydrate ligand density by ligand-exchange processes.[42]

Although gas chromatography (GC)[43] and elemental analysis (EA)[26,28] are suitable methods for determining the amount of conjugated carbohydrate on AuNPs, the sample amount that is required is about ten-fold higher than that needed for the equivalent analysis by a chemical colorimetric method.[44] With the latter method, in general, carbohydrates are reacted with phenol in the presence of sulfuric acid to give heterocyclic compounds, which are then quantified by UV spectroscopy. However, the analysis of carbohydrate derivatives by this method experienced interference by the surface plasmon band of Au from 510 to 530 nm. Thus, the anthrone method[45] (absorption at 620–630 nm) was applied to quantify the carbohydrate content on each AuNP. By using this assay, the amount of P^k ligand on each AuNP was estimated, as shown in Table 1 (see also the Supporting Information). Clearly, greater amounts

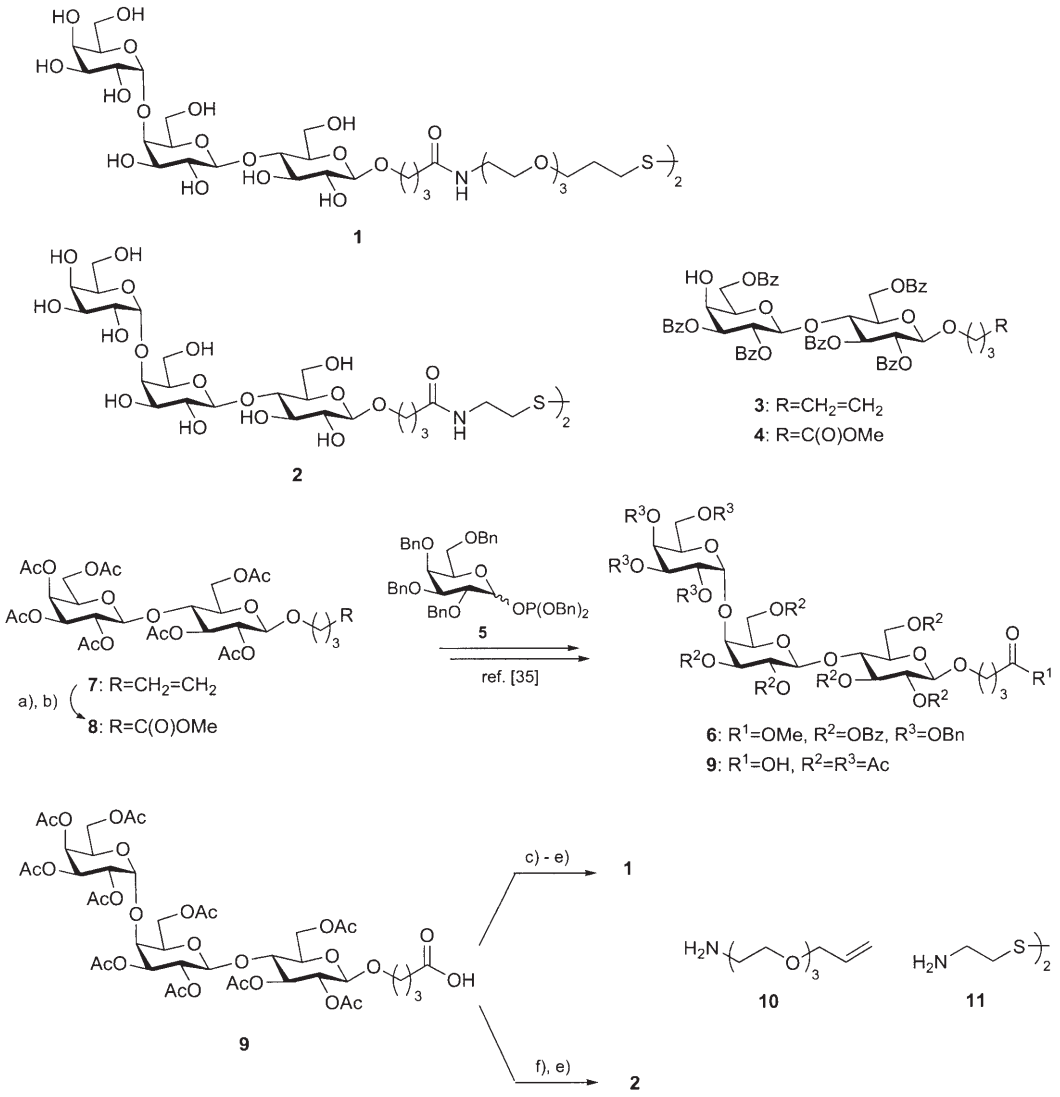

Scheme 1. Synthesis of P^k antigen. Conditions: A) $RuCl_3/NaIO_4$, $CH_2Cl_2/MeCN/H_2O$ (2:2:3); B) CH_3I, Cs_2CO_3, DMF; C) **10**, EDC, HOBt, CH_2Cl_2; D) AcSH, AIBN, MeOH; E) NaOMe, MeOH; F) **11**, EDC, HOBt, CH_2Cl_2.

of P^k were assembled on AuNPs of larger size due to the larger surface area. Further, greater amounts of P^k that have the long linker were attached to AuNPs compared with the short linker, presumably a consequence of increased net space for carbohydrate ligands; this might be the result of decreased steric hindrance when the long linker was used. The effect is more significant when the linker length was similar to that of the AuNP diameter.

Multivalent interactions of P^k-AuNPs with B-Slt

A surface plasmon resonance (SPR) competition binding assay[36,37] was used to investigate the binding affinity of the P^k ligand and various P^k-AuNPs with B-Slt.[46] Initially, thiobutanol was used as the surface matrix to fabricate a P^k-coated chip for SPR, but the P^k-AuNP aggregated on the chip surface. However, a recent report showed that the use of a short-chain methyl ethylene glycol on the AuNP surface prevented AuNP aggregation[47] and suppressed nonspecific interactions.[48] Thus, 3-[2-(2-methoxy-ethoxy)ethoxy]propane-1-thiol (MEG)[48] was used as the matrix on the chip to prevent the nonspecific interaction with P^k-AuNP.

We found that a reliable chip for the competition binding assay could be generated by forming a self-assembled monolayer by using a mixture that contained 40% thiolated P^k ligand and 60% of MEG as a matrix on a J1 biosensor chip.

The affinity of B-Slt for the P^k-functionalized chip was determined by titration with a series of B-Slt concentrations to generate multiple SPR response curves by using the rectangular hyperbolic Equation 1:[49]

$$R_{max}/R_e = 1/f\,[K_a(1/[C])] + 1 \quad (1)$$

where R_{max} is the biosensor maximum response, R_e is the corrected biosensor response at equilibrium, f is the multivalency co-relation term, C is the concentration of B-Slt, and K_a is the association constant of B-Slt with P^k. The K_a of B-Slt for this

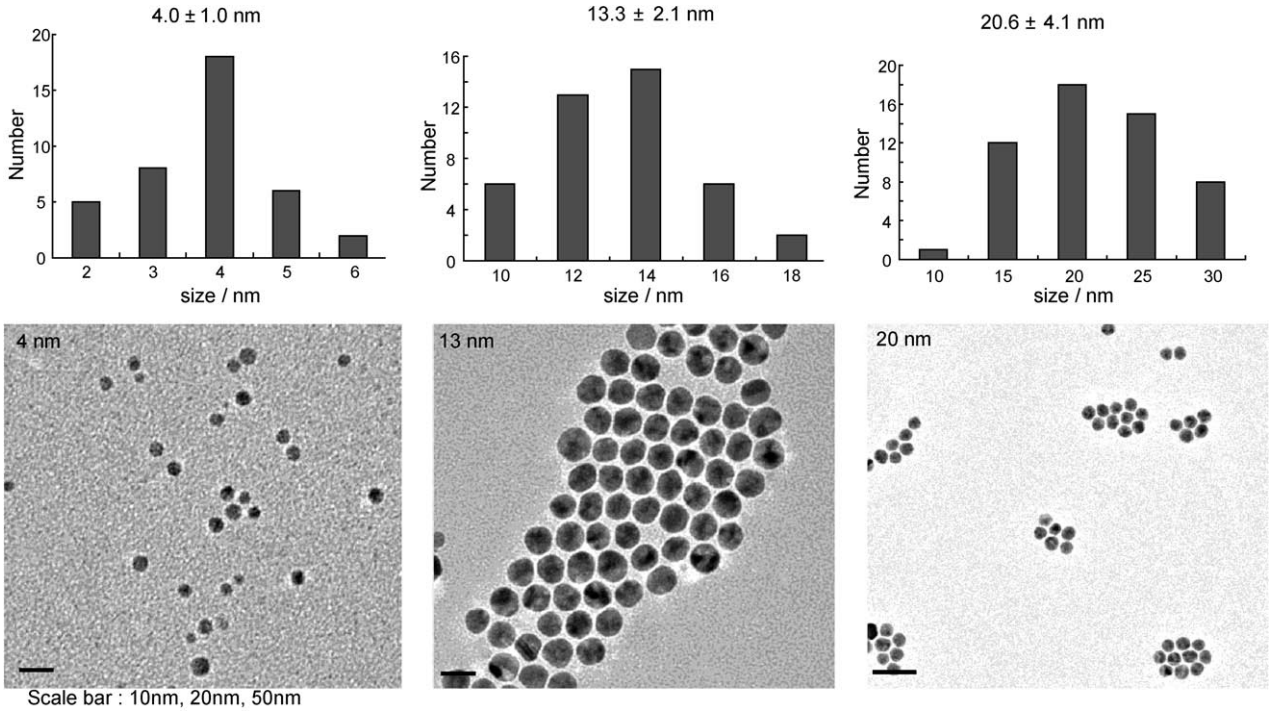

Figure 1. TEM images and size-distributions of P^k-AuNPs. Shown from left to right are: 4-P^k-s-AuNPs, 13-P^k-s-AuNPs, and 20-P^k-s-AuNPs.

chip was determined to be $1.16\times10^8\,M^{-1}$, which is similar to a reported value.[12]

In competition binding assays, 31 nM B-Slt was incubated with different concentrations of P^k ligand, P^k dimer, and P^k-AuNPs, for equilibration (1 h), then the mixture was injected into the P^k-coated Biacore chip, and binding data were collected. Figure 2 presents a typical set of SPR response curves for B-Slt competition binding with different concentrations of 4-s-P^k-AuNP.

Table 1. Number of P^k antigens per individual AuNP[a].

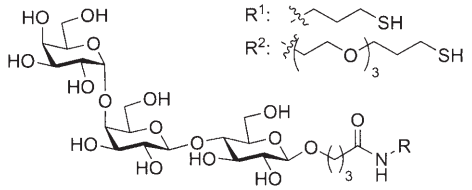

R	Size	No. of sugars per nanoparticle	Abbreviation
R^1	4 nm	60	4-P^k-s-AuNP
R^1	13 nm	826	13-P^k-s-AuNP
R^1	20 nm	1498	20-P^k-s-AuNP
R^2	4 nm	113	4-P^k-l-AuNP
R^2	13 nm	1298	13-P^k-l-AuNP
R^2	20 nm	1970	20-P^k-l-AuNP

[a] Number of P^k antigens per individual AuNP. Specifically, P^k trisaccharide with a short linker attached to NPs of 4-nm, 13-nm and 20-nm diameter are abbreviated as 4-P^k-s-AuNP, 13-P^k-s-AuNP, and 20-P^k-s-AuNP, respectively. Pk trisaccharide with a long linker attached to NPs of 4-nm, 13-nm and 20-nm diameters are abbreviated as 4-P^k-l-AuNP, 13-P^k-l-AuNP, and 20-P^k-l-AuNP, respectively. The amount of carbohydrate ligand on each individual AuNP was estimated by an anthrone test.

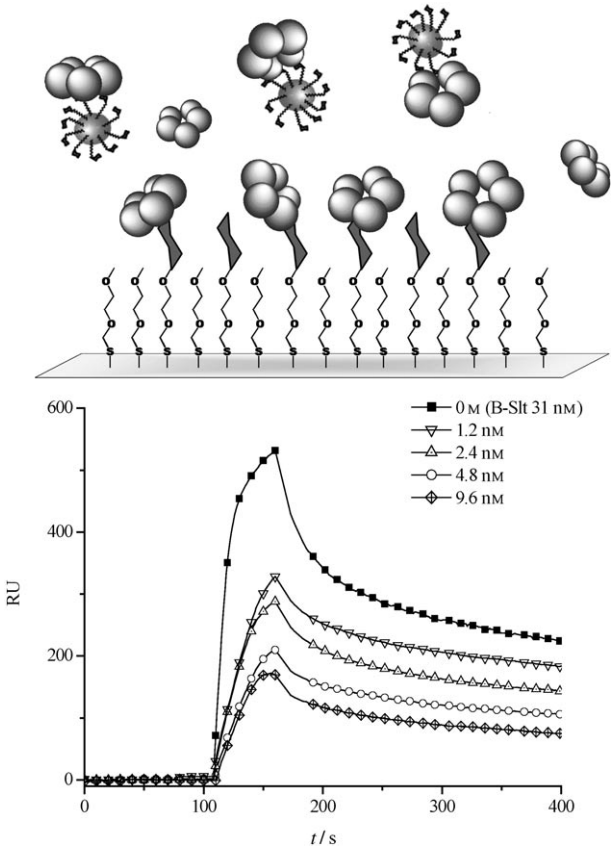

Figure 2. Inhibition of 31 nM B-Slt binding to the chip by 4-P^k-l-AuNP. A set of inhibition curves for 0, 1.2, 2.4, 4.8 and 9.6 nM 4-P^k-l-AuNP (top to bottom) is shown.

The inhibition constants (K_is) of P^k ligands were obtained by using the equations that are derived by Attie et al. [Eq. (2)],[50] and the K_i of the P^k monomer was 1.14×10^{-4} M:

$$f = [I]/\{[I] + K_i(1 + F/K_d)\} \quad (2)$$

where f is the fractional inhibition of the binding molecule, K_d is the dissociation constant of B-Slt from P^k, [I] is the antagonist concentration, K_i is the affinity of the antagonist for the B-Slt, and F is concentration of the free binding sites that are available on B-Slt. A typical K_i plot is shown in Figure 3, which was

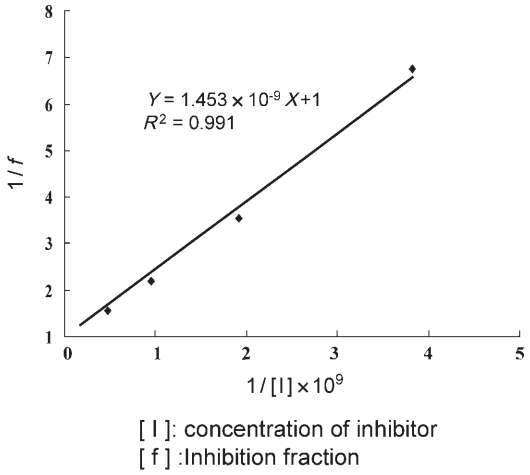

Figure 3. Double-reciprocal plot of 4-P^k-AuNP inhibiting 31 nM B-Slt binding to the chip. [I]: concentration of inhibitor; [f]: inhibition fraction.

obtained by plotting $1/f$ vs $1/[I]$. To compare the inhibition potency of the individual P^k ligand on the same AuNP with free P^k ligand, the relative inhibition avidity (RIA = K_i(inhibitor)/K_i(P^k monomer)) and relative inhibition potency (RIP = RIA/No. of P^k on AuNP) were calculated as summarized in Table 2. The more ligands that were assembled on the AuNP, the higher the affinity was. The 20-l-P^k-AuNP showed highest RIA and RIP. In comparison with free P^k, the RIA and RIP of 20-l-P^k-AuNP was 4.5×10^8 and 2.2×10^5 times greater, respectively. These inhibition results by SPR indicated that 20-l-P^k-AuNP served as an effective probe for B-Slt; it displayed superior antagonistic activity to other P^k-AuNPs, and even to a decavalent starfish inhibitor.[46]

The X-ray crystal structure of B-Slt showed[15] that it is composed of five monomers, each of which contains three P^k-binding sites (Figure S2). Site 3 is nearly perpendicular to the complex and thus contributes less to P^k binding[17,51] compared to sites 1 and 2. The distance between sites 1 and 2 is approximately 14 Å, whereas the distance between two sites 1 and two sites 2 are 27 and 29 Å, respectively. The maximum distance between two P^k ligands of the P^k dimer **2** was estimated as 26 Å (calculated based on a C–C single bond of 1.54 Å), which is too long to bind sites 1 and 2 on the same monomer, or on different monomers of B-Slt, and is too short to bind two sites 1 or 2 between two monomers, presenting 3.1 in RIA and 1.54 in RIP. However, by increasing the linker to 55 Å (calculated based on a C–O single bond of 1.44 Å) by using a flexible ethylene glycol chain, the P^k dimer **1** showed an enhanced RIA and RIP of 17.8 and 8.9, respectively (Figure S3). These data suggest that the long linker in the divalent inhibitor contributes substantially to binding to B-Slt.

We further investigated the effect of linker length on the RIA and RIP of P^k-AuNPs that bind to B-Slt. We compared the binding affinity of AuNPs (constant size) that have different length linkers; longer linkers resulted in ~5 to ~75-fold affinity enhancement. This might be due to the greater flexibility of the long linker, which makes it easier for the P^k ligand to bind the maximal number of sites of the B-Slt pentamer. In addition to linker length, ligand density and particle size also significantly influenced the RIA and RIP. We found that the binding affinity of B-Slt with the P^k-modified chip was dependent on the density of P^k on the chip surface. For example, the K_as of B-Slt for the chips that were generated by using 25% or 100% density of P^k ligand was 9.37×10^7 M^{-1} or 2.57×10^9 M^{-1}, respectively. Clearly, the K_as increased correspondingly with increased P^k ligand density on the surface. This phenomenon might be attributable to the high density of binding sites that are available per B-Slt pentamer (1.21 binding sites per nm^2). In agreement with the above observation, when the P^k density on AuNPs increased, its affinity for the B-Slt pentamer also increased. The increase in RIA for 4-l-P^k-AuNP to 4-s-P^k-AuNP was ~75-fold, whereas that for 20-l-P^k-AuNP to 20-s-P^k-AuNP was only about fivefold. The relatively lower increase in RIA for the

Table 2. The inhibition constant (K_i), relative inhibition avidity (RIA), and relative inhibition potency (RIP) of P^k-AuNPs for B-Slt. Other abbreviation are as defined for Table 1.

Compound	K_i [M]	IC_{50}	RIA[a]	RIP[b]
P^k	1.14×10^{-4}	5.11×10^{-4}	1.00	1.00
P^k-s-dimer	3.68×10^{-5}	1.65×10^{-4}	3.10	1.54
P^k-l-dimer	6.38×10^{-6}	2.86×10^{-5}	17.87	8.93
4-P^k-s-AuNP	1.46×10^{-9}	6.54×0^{-9}	78082.19	1301.36
13-P^k-s-AuNP	8.64×10^{-11}	3.87×10^{-10}	1319444.44	1597.39
20-P^k-s-AuNP	1.18×10^{-12}	5.29×10^{-12}	96610169.49	64492.77
4-P^k-l-AuNP	1.95×10^{-11}	8.74×10^{-11}	5846153.85	51735.87
13-P^k-l-AuNP	6.84×10^{-13}	3.06×0^{-12}	166666666.67	128402.67
20-P^k-l-AuNP	2.54×10^{-13}	1.14×10^{-12}	448818897.64	227826.85

[a] RIA: Relative inhibition avidity = $K_{i[inhibitor]}/K_{i[P^k]}$. [b] RIP: Relative inhibition potency = $K_{i[inhibitor]}/K_{i[P^k]}\times$No. of P^k on AuNP.

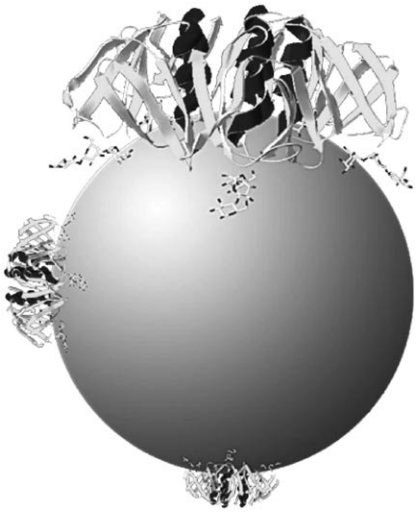

Figure 4. Relative size of AuNPs and B-Slt. Top: 4-P^k-s-AuNP to B-Slt pentamer; left: 13-P^k-s-AuNP to B-Slt pentamer; bottom: 20-P^k-s-AuNP to B-Slt pentamer.

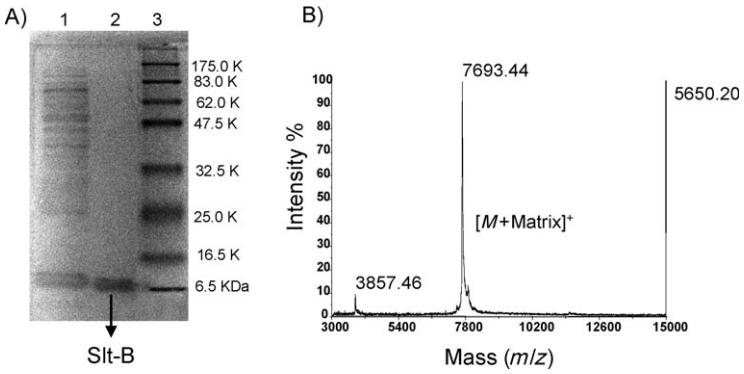

Figure 5. A) SDS-polyacrylamide gel electrophoretic analysis of B-Slt that was extracted by AuNPs. The samples were analyzed on a 15% polyacrylamide gel in the presence of 10 mM DTT. The location of B-Slt subunit band is indicated by the arrow. Lane 1, cell lysate; lane 2, after purification with AuNPs; lane 3, molecular weight marker. The apparent molecular weight of B-Slt is 7.7 kDa. B) Mass spectrum of AuNP-extracted B-Slt.

larger AuNP might be due to the binding sites (1 and 2) of B-Slt being located on a similar plane and with little curvature of this AuNP. When the AuNP surface became flatter, the ligands on the AuNP surface could interact with the binding sites more easily, as shown in Figure 4. When the AuNP size was small, the curvature of the ligand surface was significantly affected by the linker length. Thus, for the 20-nm AuNP, the enhancement of RIA and RIP upon increased linker length was less substantial compared with the values that were measured for the smaller AuNP.

P^k-AuNP as an affinity probe for the purification of B-Slt from cell lysate

Although B-Slt has been purified from recombinant *E. coli* cell lysate by using affinity chromatography, such as P1 glycoprotein or Gb_3Cer on a solid support,[52–54] Synsorb-P^k,[55] and Sepharose-P^k,[52] the extraction efficiency and tedious handling procedures needed improvement. Recently, the nitrilotriacetate-conjugated magnetic NP[56] was shown to be a better affinity particle for separation of His-tagged proteins with higher specificity and binding capacity than those of microbeads.[48,57] These results encouraged us to test P^k-AuNPs as affinity probes for B-Slt purification. The advantages of using P^k-AuNP are: 1) due to the large surface-area-to-volume ratio, the binding capacity of NPs should be higher than microbeads. 2) P^k-AuNP is soluble up to 40 mg mL^{-1} in aqueous buffers; hence AuNPs should be able to capture the target protein faster than insoluble microbeads. 3) The separation procedure is easier than that of column chromatography—AuNPs can be separated by centrifugation. 4) The P^k-AuNPs are stable in frozen solution or as a dry powder for at least 6 months.

The gene that encodes B-Slt was constructed in the high-level expression vector pJLB 28. After induction, *E. coli* that expresses recombinant B-Slt were lysed by polymyxin B,[58] and the resulting mixture was examined by sodium dodecyl sulfate polyacrylamide gel electrophoresis (SDS-PAGE). As shown in Figure 5A, lane 1, the most intensively Coomassie-blue-stained band was at ~6.5 kDa; this suggests that the major protein in the cell lysate was B-Slt (M_W of the monomer is 7693.44 Da). After extraction of B-Slt with 13-I-P^k-AuNP, only one band of ~7 kDa was observed (Figure 5A, lane 2). By native PAGE, however, a band was observed at ~35 kDa; this indicates that the pentamer complex of B-Slt is conserved after P^k-AuNP extraction (Figure S4).

The P^k-AuNP extraction complex was also analyzed directly by MALDI-TOF MS to release three peaks in the spectrum, each corresponded to the molecular weights of target protein, target protein with matrix, and target protein with two positive charges (M_W 3857.46 Da; Figure 5B); this indicates that only B-Slt was extracted by P^k-AuNP. Notably, after capturing the target protein on the AuNP surface, the normally tedious desalting procedure before mass analysis can be simplified by washing the AuNP complex with water.[35] The P^k-AuNP-captured B-Slt was resistant proteolysis by trypsin (data not shown). All of these results clearly demonstrated that P^k-AuNP is a target-specific and effective nano-affinity probe. Moreover, around 1.048 mg of B-Slt was extracted by using 50 mg P^k-AuNP (three times) from 100 mL of cell culture. The P^k-AuNP probe could be reused at least ten times without significant loss in purification performance.

SLT detection assay

Encouraged by the promising separation performance of P^k-AuNP, we then explored its potential application in the detection of Slt-I. Each Slt is composed of A and B subunits (A- and B-Slts); the A subunit attaches to the B subunit on the opposite site of the carbohydrate-binding site.[59] Thus, we developed a chip-based assay, similar to an ELISA, to detect Slt-I, as outlined schematically in Figure 6.

The monoclonal antibody against A-Slt was immobilized on a glass slide, and thus the toxin could be captured by the antibody and thereby expose the carbohydrate-binding site of B-Slt. The presence of toxin was then visualized by incubating

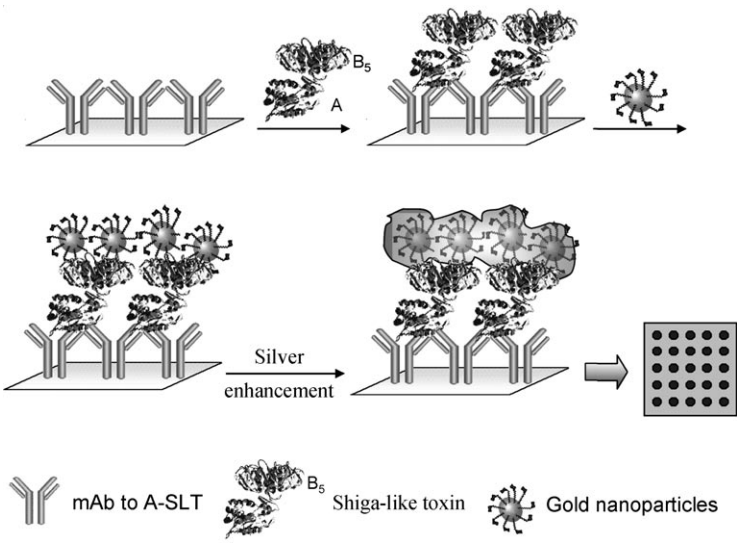

Figure 6. Schematic presentation of the chip-based assay for the detection of Slt-I. The antibody that recognizes A-Slt is immobilized on the glass slide. After being incubated with Slt-I, the presence of Slt-I on the chip is visualized by incubating the chip with the high-affinity Pk-AuNPs, followed by silver enhancement.

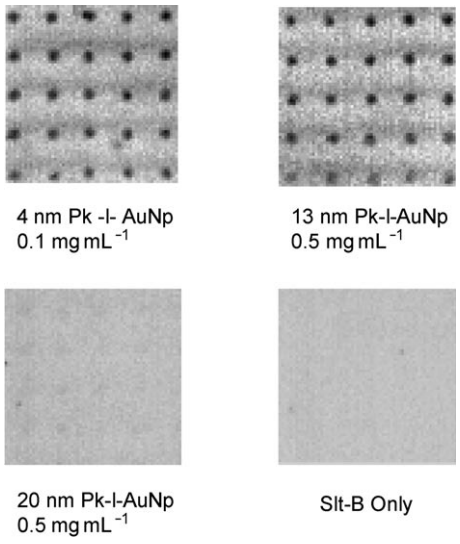

Figure 7. Effect of P^k-AuNP size on the efficiency of silver enhancement.

the chip with high-affinity P^k-AuNPs, followed by silver enhancement.[60–62] We initially investigated the influence of AuNP size on silver enhancement. B-Slt was immobilized on a *N*-hydroxysuccinimide (OSu)-activated glass slide (spot size, ca. 100 μm in diameter) by random amide bond formation by using a pin-type microarrayer.

After 1 h in a 100% humidity chamber, the glass slide was washed with phosphate-buffered saline (PBS, pH 7.4) followed by treatment with ethanolamine (50 mM, pH 8.0) to cap the unreacted *N*-hydroxysuccinimide. The capping process was performed to prevent the activated surface from reacting with target protein. For simultaneous incubation with different samples, the coated slide was divided into three detection areas by a slide incubation chamber. Then, the slide was incubated with 4-, 13-, or 20-P^k-I-AuNPs (0.5 mg mL^{-1} each, 1% BSA in PBS), respectively, for 1 h at 37 °C. The slide was washed with PBST (PBS that contained 0.05% (*w*/*v*) Tween 20, pH 7.4) and PBS alternately. After silver enhancement, the glass slide was visualized by using a plate scanner. As shown in Figure 7, small-sized AuNPs showed a better silver enhancement effect. In the silver enhancement, AuNPs serve as catalysts to reduce silver(I) ions to metallic silver, which is then deposited on the AuNP nuclei. Thus, when small-sized AuNPs were used, more particles were captured on the slide, which resulted in more nuclei being available for silver precipitation.

In the Slt-I detection assay, the monoclonal antibody against A-Slt (1 mg mL^{-1}, Abcam) was immobilized on the OSu glass slide and then divided into three detection areas, as shown in Figure 8. The left area in Figure 8 was treated with 1 μg mL^{-1} Slt-I in PBS for 1 h. After extensive washing with PBST, the protein A-conjugated 13 nm AuNPs were used as the positive control probe (Figure 8 right), and the 13-I-P^k-AuNP solution was added to the Slt-detection area (Figure 8, left). The image of the Slt-I-detection area showed positive signals for the solution that contained the target Slt-I (Figure 8, left), and a negative signal for the area without Slt-I (Figure 8, middle). The detection sensitivity (1 μg mL^{-1} Slt-I) was equivalent to that obtained by using quantum dots in an Slt-I detection assay.[63] Although the detection limit of our nonoptimized P^k-AuNP-based Slt-I detection method was not as sensitive as ELISA,[64] our method provides a relatively cost-effective, rapid and accurate platform.[65]

Conclusions

In conclusion, we present a straightforward method to prepare thiolated P^k antigen and its AuNP conjugates. By TEM image analysis and anthrone–sulfuric acid colorimetric assay, the amount of ligand on the AuNP surface could be estimated. Due the steric effects, a greater amount of P^k antigen with a long linker was assembled on the AuNP compared with the short linker. In an SPR competition assay, the P^k-AuNPs showed a high affinity for B-Slt: up to 10^8-fold in comparison with the free P^k. The IC_{50} of 20-P^k-I-AuNP was 1.14 pM (Supporting Information), which is better than the well-designed starfish-type inhibitor.[17] Although the relative inhibition potency of each P^k antigen on AuNP was increased by 2.2×10^5-fold, which is less than the starfish-type inhibitor (increased by 10^6-fold), the synthesis of P^k-coated AuNPs is relatively simple by comparison. The high affinity of P^k-AuNP for B-Slt might result from the high-density binding site of B-Slt and the low curvature of the large NP surface; this results in the binding of all B-Slt-binding sites simultaneously. Additionally, AuNPs had the advantage of increasing the relative inhibition potency by optimizing the surface density by thiol ligand exchange. Due to its high affinity for B-Slt, large surface-area-to-volume ratio, and mono-dispersion in solution, P^k-AuNPs are excellent specific probes for the purification of B-Slt. The extraction time by using P^k-AuNP was shorter and the amount of extracted protein was greater than that reported for P^k-coated microbeads. Furthermore, the

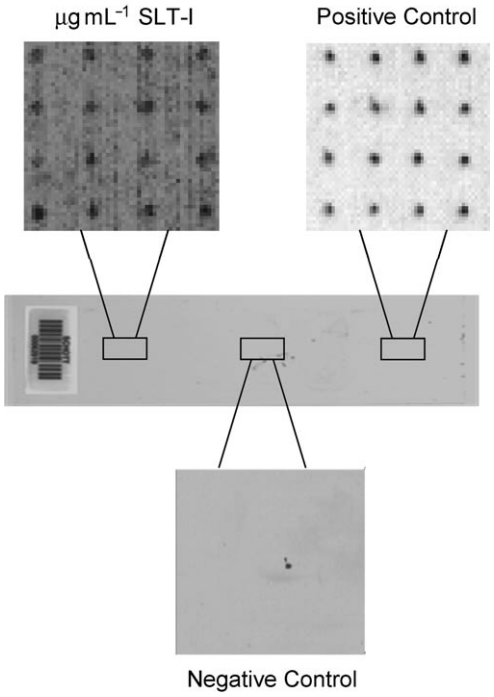

Figure 8. Silver-enhanced image of the Slt detection area.

combination of P^k-AuNP and a silver enhancement technique resulted in the development of a relatively cost-effective, rapid and accurate platform for the detection of Slt-I.

Experimental Section

3-{2-[2-(2-Amine-ethoxy)-ethoxy]}-propene (10): NaH (60% with oil, 1.5 g, 63 mmol) was added to 2-[2-(2-azido-ethoxy)ethoxy]ethanol[66] (5 g, 71 mmol) in DMF (40 mL) at 4 °C. After 30 min, allylbromide (6 mL, 63 mmol) was added, and the resulting mixture was stirred at 4 °C for 3 h. MeOH (5 mL) was then added to quench the reaction, and the solution was partitioned between H_2O and CH_2Cl_2. The aqueous layer was further extracted twice with CH_2Cl_2 and the combined organic layers were dried over $MgSO_4$. The solvent was removed under reduced pressure, and the resulting residues were purified by silica gel chromatography (EtOAc/hexanes 1:3) to afford the desired azide as oil (6 g, 88%); ^{1}H NMR (400 MHz, $CDCl_3$): δ = 5.92–5.87 (m, 1H; CH_2CH), 5.28 (d, J = 17.2 Hz, 1H; CH_2CH), 5.16 (d, J = 10.8 Hz, 1H; CH_2CH), 4.01 (d, J = 5.6 Hz, 2H; OCH_2), 3.67–3.58 (m, 11H; OCH_2CH_2O), 3.37 (brt, 2H; CH_2N); ^{13}C NMR (100 MHz, $CDCl_3$): δ = 134.69, 117.02, 72.16, 70.65, 70.64, 70.62, 69.96, 69.36, 50.63; HRMS (FAB): m/z calcd for $C_9H_{18}N_3O_3$: 216.1348; found: 216.1349 $[M+H]^+$. PPh_3 (2.5 g, 9 mmol) was added to the above compound (1 g, 5 mmol) in THF/H_2O (3:1, 16 mL) and the resulting mixture was stirred at rt for 8 h. The solvent was removed under reduced pressure, and the resulting residues were purified by silica gel chromatography (MeOH/CH_2Cl_2 1:3) to give compound **10** (700 mg, 80%); ^{1}H NMR (500 MHz, MeOH): δ = 6.01–5.95 (m, 1H; CH_2CH), 5.36 (d, J = 17.2 Hz, 1H; CH_2CH), 5.23 (d, J = 10.8 Hz, 1H; CH_2CH), 4.09 (d, J = 5.6 Hz, 2H; OCH_2), 3.72–3.58 (m, 11H; OCH_2CH_2O), 2.85 (brt, 2H; CH_2N); ^{13}C NMR (125 MHz, CD_3OD): δ = 136.29, 117.35, 73.58, 73.16, 71.69, 71.68, 71.40, 70.69, 42.27.; HRMS (FAB): m/z calcd for $C_9H_{20}NO_3$: 190.1443 $[M+H]^+$; found: 190.1446.

α-D-Galactopyranosyl-(1→4)-β-D-galactopyranosyl-(1→4)-β-D-glucopyranosyl-1-*N*-(2-{2-[2-(3-mercapto-propoxy)ethoxy]ethoxy}ethyl)-4-butyramide (1): To a solution of compounds **9** (200 mg, 0.978 mmol) and **10** in CH_2Cl_2 (20 mL) were added EDC (75 mg, 0.396 mmol) and HOBt (53 mg, 0.396 mmol) at room temperature. After stirring for 1 h, the reaction mixture was evaporated under vacuum, and the resulting residues were dissolved in EtOAc, and washed with water and brine. The organic layer was dried over $MgSO_4$ and then concentrated. The residues were purified by silica gel chromatography to give allylated compound (213 mg, 91%). R_f = 0.29 (EtOAc/hexanes + 10% MeOH 1:1); ^{1}H NMR (500 MHz, $CDCl_3$): δ = 6.45 (NH), 5.95–5.87 (m, 1H; CH_2CH), 5.57 (d, J = 2.3 Hz, 1H; H-4″), 5.38 (dd, J = 10.8 Hz, J = 2.8 Hz, 1H; H-3″), 5.27 (d, J = 17.2 Hz, 1H; CH_2CH), 5.19–5.16 (m, 3H; H-3′, H-2″, CH_2CH), 5.10 (dd, J = 10.6 Hz, J = 7.6 Hz, 1H; H-2), 4.98 (d, J = 3.2 Hz, 1H; H-1″), 4.87 (t, J = 8.3 Hz, 1H; H2′), 4.73 (dd, J = 1.8 Hz, J = 10.7 Hz, 1H; H-6b), 4.51 (d, J = 8.0 Hz, 1H; H-1′), 4.50–4.45 (m, 3H, H-3, H-5″; H-6a), 4.43 (dd, J = 7.4 Hz, J = 11.0 Hz, 1H; H-6b′), 4.18–4.07 (m, 4H; H-5, H-6a′, H-6″), 4.01 (d, J = 5.6 Hz, 2H; OCH_2), 3.93 (t, J = 6.4 Hz, 1H; H-4), 3.88–3.74 (m, 2H; H-5, H-4′), 3.65–3.61 (m, 11H; OCH_2CH_2O), 3.55 (brt, 2H; CH_2N), 3.37 (m, 2H; H-a), 2.25–2.21 (m, 2H; Hc), 2.12 (s, 3H; Ac), 2.11 (s, 3H; Ac), 2.07 (s, 3 ;, Ac), 2.06 (s, 3H; Ac), 2.05 (s, 6H; Ac), 2.04 (s, 3H; Ac), 2.03 (s, 6H; Ac), 1.97 (s, 3H; Ac), 1.94–1.81 (m, 2H; Hb); ^{13}C NMR (125 MHz, $CDCl_3$): δ = 172.78, 170.65, 170.64, 170.42, 170.06, 169.80, 169.60, 169.51, 168.83, 134.61, 117.24, 101.05, 100.58, 99.60, 76.88, 76.38, 73.05, 72.78, 72.59, 72.18, 71.81, 70.51, 70.18, 69.75, 69.36, 69.29, 68.97, 68.84, 67.89, 67.12, 67.05, 62.08, 61.30, 60.26, 39.31, 32.46, 25.61, 20.90, 20.85, 20.68, 20.67, 20.63, 20.60, 20.56, 20.49.; HRMS (FAB): m/z calcd for $C_{51}H_{76}NO_{30}$: 1182.4374 $[M+H]^+$; found: 1182.4379. The above compound (265 mg, 0.224 mmol), thiolacetic acid (0.2 mL, 3.3626 mmol), and a catalytic amount of AIBN in MeOH (20 mL) were degassed, then heated to 75 °C for 12 h. The mixture was evaporated under vacuum, and the resulting residues were purified by silica gel chromatography to give fully protected thiolate compound (211 mg, 75%). R_f = 0.30 (1:1 EtOAc/hexane + 10% MeOH); ^{1}H NMR (400 MHz, $CDCl_3$): δ = 6.45 (NH), 5.58 (d, J = 2.4 Hz, 1H; H-4″), 5.39 (dd, J = 11.2 Hz, J = 3.6 Hz, 1H; H-3″), 5.21–5.16 (m, 2H; H-3′, H-2″), 5.10 (dd, J = 10.4 Hz, J = 7.6 Hz, 1H; H-2), 4.98 (d, J = 3.6 Hz, 1H; H-1″), 4.87 (t, J = 8.4 Hz, 1H; H2′), 4.73 (dd, J = 1.8 Hz, J = 10.7 Hz, 1H; H-6b), 4.51 (d, J = 8.0 Hz, 1H; H-1′), 4.50–4.45 (m, 3H; H-3, H-5″, H-6a), 4.41 (dd, J = 7.4 Hz, J = 11.0 Hz, 1H; H-6b′), 4.19–4.08 (m, 4H; H-5, H-6a′, H-6″), 4.01 (d, J = 5.6 Hz, 2H; OCH_2), 3.93 (t, J = 6.4 Hz, 1H; H-4), 3.88–3.74 (m, 2H; H-5, H-4′), 3.65–3.55 (m, 11H; OCH_2CH_2O), 3.51 (brt, 2H; CH_2N), 3.45 (m, 2H), 2.95 (t, J = 7.2 Hz , 2H; Ha), 2.32 (s, 3H; SAc), 2.26–2.25 (m, 2H; Hc), 2.12 (s, 3H; Ac), 2.11 (s, 3H; Ac), 2.08 (s, 3H; Ac), 2.07 (s, 3H; Ac), 2.06 (s, 6H; Ac), 2.05 (s, 3H; Ac), 2.04 (s, 6H; Ac), 1.98 (s, 3H; Ac), 1.90–1.82 (m, 2H; Hb); ^{13}C NMR (100 MHz, $CDCl_3$): δ = 195.88, 172.71, 170.65, 170.64, 170.42, 170.06, 169.80, 169.60, 169.51, 168.83, 101.05, 100.58, 99.60, 76.88, 76.38, 73.04, 72.77, 72.57, 71.76, 70.49, 70.45, 70.19, 70.13, 69.78, 69.55, 69.31, 68.95, 68.82, 67.87, 67.10, 67.04, 62.06, 61.26, 60.25, 39.28, 32.50, 30.60, 29.50, 25.90, 25.59, 20.90, 20.86, 20.68, 20.67, 20.63, 20.60, 20.56, 20.49.; HRMS (FAB): m/z calcd for $C_{53}H_{79}NO_{31}SNa$: 1280.4357 $[M+Na]^+$; found: 1280.4361. A catalytic amount of NaOMe was added to a solution of the above compound (100 mg, 0.079 mmol) in MeOH (15 mL). The mixture was stirred at room temperature for 30 min. The mixture was diluted with MeOH and then treated with IR-120 H^+ resin. Resins were filtered off, the filtrate was concentrated under vacuum, and the resulting residues were purified by P2 gel column by using distilled water as the eluent to give compound **1** in 92% yield; ^{1}H NMR (500 MHz, CD_3OD): δ = 4.91 (d, J = 3.5 Hz, 1H), 4.38 (d, J = 6.5 Hz, 1H), 4.26–4.20 (m, 2H), 3.95–3.45 (m, 36H),

3.37–3.32 (m, 4H), 3.20–3.15 (m, 2H), 2.29 (t, $J=7.3$ Hz, 2H), 1.87 (t, $J=6.5$ Hz, 2H), 1.81 (t, $J=6.5$ Hz, 2H), 1.29–1.25 (m, 4H); ^{13}C NMR (125 MHz, CD_3OD): $\delta=105.52$, 104.39, 102.84, 81.16, 79.92, 76.68, 76.57, 75.04, 74.82, 72.99, 72.81, 71.73, 71.69, 71.43, 71.41, 71.35, 71.33, 71.19, 70.71, 70.42, 70.27, 70.08, 70.04, 40.54, 36.22, 35.08, 33.81, 30.88, 30.43, 27.32, 21.91; HRMS (FAB): *m/z* calcd for $C_{62}H_{121}N_2O_{40}S_2$ 1597.6160 $[M]^+$; found: 1597.5871.

Synthesis of P^k-AuNPs: All glassware used in the following reaction was cleaned by the Pirahna reagent (concd. H_2SO_4/30% hydrogen peroxide 3:1) and repeatedly rinsed with deionized water. Gold particles of 4-nm diameter were synthesized in deionized water by the addition of $NaBH_4$ (0.2 mL, 0.5 mg mL^{-1}) to a solution of $HAuCl_4$ (3 mg) and P^k trisaccharide antigen **2** (3 mg) in deionized water (20 mL). The reaction was vigorously stirred at 4 °C for 3 h. The solution color changed from light-yellow to brown. The solution was stirred for another 1 h, and then most of the solvent was removed under vacuum until only a small amount of water remained. The resulting P^k-AuNP solution was centrifuged at 55000 *g* for 1.5 h to separate the P^k-AuNPs from free P^k. The supernatant was discarded, and the residue was redispersed in deionized water (1 mL). The centrifugation and redispersion steps were repeated three times to ensure that all of the free ligand was removed. The typical solution of 4-nm AuNPs in deionized water had a characteristic absorption band at 512–515 nm.

P^k-AuNPs of 13-nm size were prepared by using trisodium citrate to reduce $HAuCl_4$. A freshly prepared solution of trisodium citrate (10 mL, 10 mg mL^{-1} in deionized water) was added quickly to a boiling $HAuCl_4$ solution (190 mL, 0.05 mg mL^{-1} in deionized water). After the solution color changed from pale-yellow to wine-red, the mixture was stirred at refluxing temperature for another 15 min and then allowed to cool to room temperature. This solution was degassed under vacuum for 30 s^{-1}, and bubbled with nitrogen for several cycles to remove oxygen. After degasification, the reduced P^k antigen (1 mL, 10 mg mL^{-1}) was added while stirring at room temperature. After stirring overnight, the solvent was removed under vacuum until a small amount of water remained. The resulting P^k-AuNP solution was centrifuged at 14000 *g* for 0.5 h to separate the P^k-AuNPs from free P^k. After discarding the supernatant, the residue was redispersed with deionized water (1 mL). The centrifugation and redispersion steps were repeated three times to ensure that all of the free ligand was removed. The typical solution of 13-nm AuNP in deionized water had a characteristic absorption band at 518–520 nm.

The synthesis of 20-nm AuNPs was similar as that described for the synthesis of 13 nm AuNPs. However, the $HAuCl_4$ concentration was increased to 0.1 mg mL^{-1}. After addition of trisodium citrate, the solution color changed to deep red. The NPs were collected by centrifugation at 12000 *g*. The typical solution of 20-nm AuNP in deionized water had a characteristic absorption band at 522–525 nm.

Transmission electron microscopy (TEM) measurements: Transmission electron microscopy was preformed on a JEOL microscope (Model JEM-2011) that operated at 200 kV to characterize the size and dispersion of the NPs. A drop of the NP solution (1 μL) was placed on a carbon-coated 200-mesh copper grid. The grid was left to dry at room temperature for several hours, and then subsequently dried under vacuum overnight and analyzed. Mean particle size and standard deviation were determined by measuring at least 50 particles.

Determination of carbohydrate amount on nanoparticles surface: Glyconanoparticles (100–500 μg) were dispersed in deionized water (0.5 mL) in an ice bath. A freshly prepared 0.5% (*w/w*) solution of anthrone in sulfuric acid (1 mL) was added slowly to this solution. The resulting solution was gently mixed and heated to 100 °C for 10 min. The absorption of the solution was measured at 620 nm and compared with those that were obtained from a standard curve to determine the amount of ligand on the AuNP surface.

SPR measurements: The affinity between glyconanoparticles and B-Slt was measured by using a BIAcore 3000 (BIAcore AB, Uppsala, Sweden). The J1 sensor chip was modified with P^k antigen by injecting a mixture that contained 40% P^k antigen and 60% 3-[2-(2-methoxy-ethoxy)ethoxy]propane-1-thiol for 15 min (1 μL min^{-1}) three times. The SPR responses for the P^k antigen were about 300–500 R.U. The affinity between this chip and B-Slt was determined by injecting a series of B-Slt concentrations to generate multiple SPR response curves, to calculate the K_a of B-Slt. In the competition assay, the SPR response curves of inhibitor were obtained by injecting a mixture of 31-nM B-Slt with various concentrations of competitive inhibitor into a P^k-antigen-modified J1 chip. The inhibition constant (K_i) was obtained by using Equation (2).

Purification of B-Slt by P^k-AuNP: *E. coli* that carried the B-Slt gene (encoded in plasmid pJLB 28) was obtained from Professor Brunton[67] and was cultured in LB Broth medium (500 mL) that contained ampicillin (100 μg mL^{-1}) for 3 h at 37 °C. Isopropyl β-D-thiogalactoside (IPTG) was added to the growing cells (OD = 0.5) to a final concentration at 1 mM, and the strains were cultured for an additional 4 h at 37 °C. The cells were harvested by centrifugation at 6000 *g* for 10 min at 4 °C, and the pellet was washed with 0.9% NaCl. The cells were lysed by incubation of the above pellet in PBS (10 mL) that contained polymyxin B sulfate (0.1 mg mL^{-1}) with shaking at 300 rpm at 37 °C for 30 min. The cell lysates were centrifuged at 12000 *g* for 10 min, and the supernatant was recovered. The pellet was extracted with polymyxin B solution (5 mL), and the supernatants were combined. 13-P^k-s-AuNP (50 mg) was added to a cell lysate (1 mL), and then the mixture was gently shaken (60 rpm) for 10 min. The P^k-AuNP-protein complex was centrifuged at 14400 *g* at 4 °C for 15 min, and the precipitates were washed with PBS (3 × 1 mL). B-Slt was eluted by 6 M $MgCl_2$ (in deionized water), and the eluent was dialyzed against PBS. Protein concentration was determined by using a Bradford protein assay kit (Bio-Rad). After eluting with 6 M $MgCl_2$, the AuNP was recovered by centrifugation and by washing the precipitate with deionized H_2O. The purity of purified B-Slt was examined by 15% SDS-PAGE and MALDI-TOF mass analysis.

Slt detection assay: The *N*-hydroxysuccinimide-activated glass slide was spotted with a monoclonal antibody (Abcam, Inc. Cambridge, UK) against A-Slt. The slide was incubated at 4 °C for 1 h, and then washed with PBS twice. Ethanolamine (50 mM in deionized water, pH 8) was used as a blocking reagent to cap the activated esters. Then, Slt-I (20 μL, 1 μg mL^{-1}, Merck) was dropped onto the antibody-coated slide surface followed by gentle shaking at room temperature for 1 h. The slide was washed three times with PBS. The 13-P^k-s-AuNP was incubated with the slide and allowed to be captured by exposed B-Slt. Finally, silver enhancement was performed by applying silver staining solution (500 μL, Sigma) to the dried slide for 8 min. The reaction was terminated by washing the slide with $Na_2S_2O_4$ (50 mM). The slides were spin-dried and imaged with a plate scanner.

Acknowledgements

This work was financially supported by the National Tsing Hua University, Academia Sinica, and National Science Council, Taiwan.

Keywords: glycoconjugates · multivalent interaction · P^k antigen · Shiga-like toxin · surface plasmon resonance

[1] C. R. Bertozzi, L. L. Kiessling, *Science* **2001**, *291*, 2357–2364.
[2] M. Mammen, S.-K. Choi, G. M. Whitesides, *Angew. Chem.* **1998**, *110*, 2908–2953; *Angew. Chem. Int. Ed.* **1998**, *37*, 2754–2794.
[3] L. L. Kiessling, J. E. Gestwicki, L. E. Strong, *Curr. Opin. Chem. Biol.* **2000**, *4*, 696–703.
[4] J. E. Gestwicki, C. W. Cairo, L. E. Strong, K. A. Oetjen, L. L. Kiessling, *J. Am. Chem. Soc.* **2002**, *124*, 14922–14933.
[5] R. Roy, J. M. Kim, *Angew. Chem.* **1999**, *111*, 380–384; *Angew. Chem. Int. Ed.* **1999**, *38*, 369–372.
[6] M. D. Disney, J. Zheng, T. M. Swager, P. H. Seeberger, *J. Am. Chem. Soc.* **2004**, *126*, 13343–13346.
[7] J. E. Kingery-Wood, K. W. Williams, G. B. Sigal, G. M. Whitesides, *J. Am. Chem. Soc.* **1992**, *114*, 7303–7305.
[8] K. Hanaoka, T. J. Pritchett, S. Takasaki, N. Kochibe, S. Sabesan, J. C. Paulson, A. Kobata, *J. Biol. Chem.* **1989**, *264*, 9842–9849.
[9] P. A. Clemons, *Curr. Opin. Chem. Biol.* **1999**, *3*, 112–115.
[10] L. L. Kiessling, J. E. Gestwicki, L. E. Strong, *Angew. Chem.* **2006**, *118*, 2408–2429; *Angew. Chem. Int. Ed.* **2006**, *45*, 2348–2368.
[11] M. A. Karmali, M. Petrie, C. Lim, P. C. Fleming, G. S. Arbus, H. Lior, *J. Infect. Dis.* **1985**, *151*, 775–782.
[12] M. Naiki, D. M. Marcus, *Biochem. Biophys. Res. Commun.* **1974**, *60*, 1105–1111.
[13] T. Waddell, S. Head, M. Petric, A. Cohen, C. Lingwood, *Biochem. Biophys. Res. Commun.* **1988**, *152*, 674–679.
[14] A. A. Lindberg, J. E. Brown, N. Strömberg, M. Westling-Ryd, J. E. Schultz, K.-A. Karlsson, *J. Biol. Chem.* **1987**, *262*, 1779–1785.
[15] H. Ling, A. Boodhoo, B. Hazes, M. D. Cummings, G. D. Armstrong, J. L. Brunton, R. J. Read, *Biochemistry* **1998**, *37*, 1777–1788.
[16] E. Fan, Z. Zhang, W. E. Minke, Z. Hou, C. L. M. J. Verlinde, W. G. J. Hol, *J. Am. Chem. Soc.* **2000**, *122*, 2663–2664.
[17] P. I. Kitov, J. M. Sadowska, G. Mulvey, G. D. Armstrong, H. Ling, N. S. Pannu, R. J. Read, D. R. Bundle, *Nature* **2000**, *403*, 669–672.
[18] J. J. Lundquist, S. D. Debenham, E. J. Toone, *J. Org. Chem.* **2000**, *65*, 8245–8250.
[19] G. L. Mulvey, P. Marcato, P. I. Kitov, J. Sadowska, D. R. Bundle, G. D. Armstrong, *J. Infect. Dis.* **2003**, *187*, 640–649.
[20] D. W. Acheson, G. T. Keusch, M. Lightowlers, A. Donohue-Rolfe, *J. Infect. Dis.* **1990**, *161*, 134–137.
[21] A. Donohue-Rolfe, M. A. Kelley, M. Bennish, G. T. Keusch, *J. Clin. Microbiol.* **1986**, *24*, 65–68.
[22] J. C. Paton, A. W. Paton, *Clin. Microbiol. Rev.* **1998**, *11*, 450–479.
[23] C. M. Niemeyer, *Angew. Chem.* **2001**, *113*, 4254–4287; *Angew. Chem. Int. Ed.* **2001**, *40*, 4128–4158.
[24] M. Mrksich, *Chem. Soc. Rev.* **2000**, *29*, 267–273.
[25] C. J. Love, L. A. Estroff, J. K. Kriebel, R. G. Nuzzo, G. M. Whitesides, *Chem. Rev.* **2005**, *105*, 1103–1169.
[26] J. M. de La Fuente, A. G. Barrientos, T. C. Rojas, J. Rojo, J. Canada, A. Fernandez, S. Penadés, *Angew. Chem.* **2001**, *113*, 2317–2321; *Angew. Chem. Int. Ed.* **2001**, *40*, 2257–2261.
[27] H. Otsuka, Y. Akiyama, Y. Kagasaki, K. Kataoka, *J. Am. Chem. Soc.* **2001**, *123*, 8226–8230.
[28] B. Nolting, J.-J. Yu, G.-Y. Liu, S.-J. Cho, S. Kauzlarich, J. Gervay-Hague, *Langmuir* **2003**, *19*, 6465–6473.
[29] D. C. Hone, A. H. Haines, D. A. Russell, *Langmuir* **2003**, *19*, 7141–7144.
[30] A. Carvalho de Souza, K. M. Halkes, J. D. Meeldijk, A. J. Verkleij, J. F. G. Vliegenthart, J. P. Kamerling, *ChemBioChem* **2005**, *6*, 828–831.
[31] S. A. Svarovsky, Z. Szekely, J. J. Barchi, Jr., *Tetrahedron: Asymmetry* **2005**, *16*, 587–598.
[32] For a recent review on gold glyconanoparticles, see: J. M. de la Fuente, S. Penadés, *Biochim. Biophys. Acta Gen. Subj.* **2006**, *1760*, 636–651.
[33] C.-C. Lin, Y.-C. Yeh, C.-Y. Yang, C.-L. Chen, G.-F. Chen, C.-C. Chen, Y.-C. Wu, *J. Am. Chem. Soc.* **2002**, *124*, 3508–3509.
[34] C.-C. Lin, Y.-C. Yeh, C.-Y. Yang, G.-F. Chen, Y.-C. Chen, Y.-C. Wu, C.-C. Chen, *Chem. Commun.* **2003**, 2920–2921.
[35] Y.-J. Chen, S.-H. Chen, Y.-Y. Chien, Y.-W. Chang, Y. H.-K. Liao, C.-Y. Chang, M.-D. Jan, K.-T. Wang, C.-C. Lin, *ChemBioChem* **2005**, *6*, 1169–1173.
[36] D. A. Mann, M. Kanai, D. J. Maly, L. L. Kiessling, *J. Am. Chem. Soc.* **1998**, *120*, 10575–10582.
[37] L. Nieba, A. Krebber, A. Pluckthun, *Anal. Biochem.* **1996**, *234*, 155–165.
[38] S.-Y. Hsieh, M.-D. Jan, L. N. Patkar, C.-T. Chen, C.-C. Lin, *Carbohydr. Res.* **2005**, *340*, 49–57.
[39] T. Buskas, E. Söderberg, P. Konradsson, B. Fraser-Reid, *J. Org. Chem.* **2000**, *65*, 958–963.
[40] M. Brust, M. Walker, D. Bethell, D. J. Schiffrin, R. J. C. S. Whyman, *J. Chem. Soc. Chem. Commun.* **1994**, 801–802.
[41] C. de Roe, P. J. Courtoy, P. Baudhuin, *J. Histochem. Cytochem.* **1987**, *35*, 1191–1198.
[42] A. Verma, V. M. Rotello, *Chem. Commun.* **2005**, 303–312.
[43] A. C. de Souza, K. M. Halkes, J. D. Meeldijk, A. J. Verkleij, J. F. G. Vliegenthart, J. P. Kamerling, *Eur. J. Org. Chem.* **2004**, 4323–4339.
[44] H. Scherz, G. Bonn in *Analytical Chemistry of Carbohydrates*, Thieme, Stuttgart, **1998**.
[45] L. H. Koehler, *Anal. Chem.* **1952**, *24*, 1576–1579.
[46] V. Kanda, P. Kitov, D. R. Bundle, M. T. McDermott, *Anal. Chem.* **2005**, *77*, 7497–7504.
[47] M. Zheng, X. Huang, *J. Am. Chem. Soc.* **2004**, *126*, 12047–12054.
[48] P.-C. Lin, P.-H. Chou, S.-H. Chen, H.-K. Liao, K.-Y. Wang, Y.-J. Chen, C.-C. Lin, *Small* **2006**, *2*, 485–489.
[49] N. L. Kalinin, L. D. Ward, D. J. Winzor, *Anal. Biochem.* **1995**, *228*, 238–244.
[50] A. D. Attie, R. T. Raines, *J. Chem. Educ.* **1995**, *72*, 119–124.
[51] P. I. Kitov, D. R. Bundle, *J. Am. Chem. Soc.* **2003**, *125*, 16271–16284.
[52] H. Nakajima, Y. U. Katagiri, N. Kiyokawa, T. Taguchi, T. Suzuki, T. Sekino, K. Mimori, M. Saito, H. Nakao, T. Takeda, J. Fujimoto, *Protein Expression Purif.* **2001**, *22*, 267–275.
[53] S. Miyashita, Y. Matsuura, D. Miyamoto, Y. Suzuki, Y. Imai, *Glycoconjugate J.* **1999**, *16*, 697–705.
[54] J. Boulanger, M. Huesca, S. Arab, C. A. Lingwood, *Anal. Biochem.* **1994**, *217*, 1–6.
[55] G. Palombo, M. Rossi, G. Cassani, G. Fassina, *J. Mol. Recognit.* **1998**, *11*, 247–249.
[56] C. Xu, K. Xu, H. Gu, X. Zhong, Z. Guo, R. Zheng, X. Zhang, B. Xu, *J. Am. Chem. Soc.* **2004**, *126*, 3392–3393.
[57] P.-H. Chou, S.-H. Chen, H.-K. Liao, P.-C. Lin, G.-R. Her, A. C.-Y. Lai, C.-C. Lin, Y.-J. Chen, *Anal. Chem.* **2005**, *77*, 5990–5997.
[58] M. Karmali, M. Petric, C. Lim, R. Cheung, G. E. Arbus, *J. Clin. Microbiol.* **1985**, *22*, 614–619.
[59] P. E. Stein, A. Boodhoo, G. J. Tyrrell, J. L. Brunton, R. J. Read, *Nature* **1992**, *355*, 748–750.
[60] J. M. Nam, C. S. Thaxton, C. A. Mirkin, *Science* **2003**, *301*, 1884–1886.
[61] C. S. Holgate, P. Jackson, P. N. Cowen, C. C. Bird, *J. Histochem. Cytochem.* **1983**, *31*, 938–944.
[62] S. Gupta, S. Huda, P. K. Kilpatrick, O. D. Velev, *Anal. Chem.* **2007**, *79*, 3810–3820.
[63] E. R. Goldman, A. R. Clapp, G. P. Anderson, H. T. Uyeda, J. M. Mauro, I. L. Medintz, H. Mattoussi, *Anal. Chem.* **2004**, *76*, 684–688.
[64] K. S. Kehl, P. Havens, C. E. Behnke, D. W. Acheson, *J. Clin. Microbiol.* **1997**, *35*, 2051–2054.
[65] V. L. Tesh, J. A. Burris, J. W. Owens, V. M. Gordon, E. A. Wadolkowski, A. D. O'Brien, J. E. Samuel, *Infect. Immun.* **1993**, *61*, 3392–3402.
[66] B. C. Roy, M. Santon, S. Mallik, A. D. Campiglia, *J. Org. Chem.* **2003**, *68*, 3999–4007.
[67] A. Huang, S. de Grandis, J. Friesen, M. Karmali, M. Petric, R. Congi, J. L. Brunton, *J. Bacteriol.* **1986**, *166*, 375–379.

Received: October 4, 2007
Published online on April 8, 2008

